International Journal of Water Resources and Environmental Engineering Vol. 4(12), pp. 363-376, December 2012
Available online at http://www.academicjournals.org/IJWREE
DOI: 10.5897/IJWREE11.120
ISSN 2141-6613 ©2012 Academic Journals

Full Length Research Paper

Flow and contaminant transport simulations of the Solimões River using three depth-averaged two-equation closure turbulence models

Liren Yu[1,2]

[1]Environmental Software and Digital Visualization (ESDV), Rua Dona Maria Jacinta 482, 13561-120, São Carlos, SP, Brazil.
[2]Association of United Schools-Higher Education Center of São Carlos (ASSER-CESUSC), São Carlos 13574-380, Brazil. E-mail: lirenyu@yahoo.com.

Accepted 2 October, 2012

This paper reports a numerical simulation in the Amazon water system, aiming to develop a quasi-3D numerical tool for refinedly modeling turbulent flows and passive mass transport phenomena in natural waters. Three depth-averaged two-equation closure turbulence models, $\tilde{k}$ - $\tilde{\varepsilon}$, $\tilde{k}$ - $\tilde{w}$, and $\tilde{k}$ - $\tilde{\omega}$, were used to close the non-simplified quasi three-dimensional hydrodynamic fundamental governing equations. The discretized equations were solved by advanced multi-grid iterative method under non-orthogonal body-fitted coarse and fine grids with collocated variable arrangement. Except for steady flow computation, the processes of contaminant inpouring and plume development at the beginning of discharge, caused by a side-discharge of a tributary, also have been numerically investigated. The used three depth-averaged two-equation closure models are all suitable for modeling strong mixing turbulence. The newly established turbulence model, such as $\tilde{k}$ - $\tilde{\omega}$ model with higher order of magnitude of transported variable $\tilde{\omega}$, provides a possibility to crease the computational precision.

Key words: River modeling, numerical modeling, contaminant transport, depth-averaged turbulence models, multi-grid iterative method.

INTRODUCTION

Almost all flows in natural rivers are turbulence. Dealing with the problems of turbulence related tightly to stream pollutions is challenging both for scientists and engineers, because of their damaging effect on our limited water resources and fragile environment. It is important to develop adequate mathematical models, turbulence models, numerical methods and corresponding analytical tools for timely simulating and predicting transport behaviors in artificial and natural waters.

Although the significance of modeling turbulent flows and transport phenomena with a high precision is clear, the numerical simulation and prediction for natural waters with complex geometry and variable bottom topography are still unsatisfied. This is mainly due to the inherent complexity of the problems being considered. Any computation and simulation of flow and transport processes depends critically on the following four elements: to generate a suitable computational domain with the ability to deal with non-regular geometrical boundaries, such as riversides and island boundaries; to establish applicable turbulence models; to adopt efficient algorithms, and to develop corresponding numerical tool.

Quasi three-dimensional hydrodynamic models are frequently used for modeling in shallow and well-mixed waters. However, many models used in practice merely consider the turbulent viscosity and diffusivity through constants or through simple phenomenological algebraic formulas (Choi and Takashi, 2000; Lunis et al., 2004; Vasquez, 2005; Kwan, 2009), which are to a great degree estimated according to the modeller's experience. Although other practical quasi three-dimensional hydrodynamic models are really closed by depth-averaged two-equation closure turbulence model, they almost all concentrate on the investigations and applications

of depth-averaged $\tilde{k}$ - $\tilde{\varepsilon}$ model (Rodi et al., 1980; Chapman and Kuo, 1982; Mei et al., 2002; Johnson et al., 2005; Cea et al., 2007; Hua et al., 2008; Kimura et al., 2009; Lee et al., 2011), appeared already beyond 30 years. It is well known that the order of magnitude of transported variable $\tilde{\varepsilon}$ for $\tilde{k}$ - $\tilde{\varepsilon}$ model is very low.

Recent development of turbulence model theory has provided more realistic and advanced turbulence models. From an engineering perspective, two-equation closure models can establish a higher standard for numerically approximation of main flow behaviors and transport phenomena in terms of efficiency, extensibility and robustness (Yu and Righetto, 1998). However, the most common standard two-equation closure models, used widely in industry, cannot be directly employed in quasi three-dimensional modeling. The depth-averaged versions of corresponding turbulence models should be established in advance.

Except for the classical depth-averaged $\tilde{k}$ - $\tilde{\varepsilon}$ model closure, current simulations still adopt the closures of depth-averaged $\tilde{k}$ - $\tilde{w}$ model and of depth-averaged $\tilde{k}$ - $\tilde{\omega}$ model, respectively. The depth-averaged $\tilde{k}$ - $\tilde{\omega}$ model was stemmed from the most common standard *k-ω* model, originally introduced by Saffman (1970) but popularized by Wilcox (1998). The results, computed by the three depth-averaged two-equation closure turbulence models, were compared each other in the paper. Such example, however, hardly exists for the simulation of contaminant transport in natural waters. Modeling by using different two-equation closure approaches certainly increases the credibility of simulation results (Yu and Yu, 2009).

On the other hand, recent advancements in grid generation techniques, numerical methods and IT techniques have provided suitable approaches to generate non-orthogonal boundary-fitted coordinates with collocated grid arrangement, on which the non-simplified hydrodynamic fundamental governing equations can be solved by multi-grid iterative method (Ferziger and Peric, 2002). This paper describes a quasi three-dimensional hydrodynamic simulation of flow and transport in a multi-connected domain, with the aim of developing the *grid-generator*, *flow-solver* and *interface* of a software. The developed software, namely Q3drm1.0 by the author, provides three selectable depth-averaged two-equation closure turbulence models and can solve quasi three-dimensional refined flow and transport phenomena in complex artificial and natural waters.

HYDRODYNAMIC FUNDAMENTAL GOVERNING EQUATIONS

The complete, non-simplified fundamental governing equations of quasi three-dimensional computation, in terms of coordinate-free vector forms derived by using vertical Leibniz integration for a Control Volume (CV, an arbitrary quadrilateral with center point *P*), considering the variation of the bottom topography and water surface and neglecting minor terms in the depth-averaging procedure, can be written as follows:

$$\frac{\partial}{\partial t}\int_{\Omega}\rho h\bar{\phi}d\Omega+\int_{S}\rho h\bar{\phi}\vec{v}\bullet\vec{n}dS=\int_{S}\Gamma h\mathbf{grad}\bar{\phi}\bullet\vec{n}dS+\int_{\Omega}\bar{q}_{\phi}d\Omega \quad (1)$$

where Ω is the CV's volume; S is the face; $\vec{v}$ is the depth-averaged velocity vector, the superscript " $-$ " indicates that the value is strictly depth-averaged; $\bar{\phi}$ is any depth-averaged conserved intensive property (for mass conservation, $\bar{\phi}=1$; for momentum conservation, $\bar{\phi}$ is the components in different directions of $\vec{v}$; for conservation of a scalar, $\bar{\phi}$ is the conserved property per unit mass); Γ is the diffusivity for the quantity $\bar{\phi}$; $\bar{q}_{\phi}$ denotes the source or sink of $\bar{\phi}$; and *h* and ρ are local water depth at *P* and density, respectively.

For the momentum conservation of Equation (1), Γ = $\tilde{\mu}_{\text{eff}}$ (depth-averaged effective viscosity); for temperature or concentration transport, $\Gamma=\tilde{\Gamma}_{\phi,\text{t}}$ (temperature or concentration diffusivity), where the superscript "~" indicates the quantity characterizing depth-averaged turbulence. The source (sink) term $\bar{q}_{\phi}$ for momentum conservation may include surface wind shear stresses, bottom shear stresses, pressure terms and additional point sources (or point sinks).

The continuity and momentum equations as well as the transport equation of the scalar $\bar{\phi}$ have been reported in details by Yu and Yu (2009).

DEPTH-AVERAGED TURBULENCE CLOSURE MODELS

The depth-averaged effective viscosity $\tilde{\mu}_{\text{eff}}$ and diffusivity $\tilde{\Gamma}_{\phi,\text{t}}$, appeared in Equation (1), are dependent on the molecular dynamic viscosity μ and depth-averaged eddy viscosity $\tilde{\mu}_{\text{t}}$: $\tilde{\mu}_{\text{eff}}=\mu+\tilde{\mu}_{\text{t}}$ and $\tilde{\Gamma}_{\phi,\text{t}}=\tilde{\mu}_{\text{t}}/\sigma_{\phi,\text{t}}$, where $\sigma_{\phi,\text{t}}$ is the turbulence Prandtl number for temperature diffusion or Schmidt number for concentration diffusion, and $\tilde{\mu}_{\text{t}}$ is a scalar property and normally determined by two extra transported variables.

The used first two-equation turbulence model for depth-averaged calculation was suggested by McGuirk and Rodi as early as in 1977:

$$\frac{\partial(\rho h\tilde{k})}{\partial t}+div(\rho h\tilde{k}\vec{v})=div(h(\mu+\frac{\tilde{\mu}_t}{\sigma_k})\mathbf{grad}\tilde{k})+hP_k-\rho h\tilde{\varepsilon}+\rho hP_{kv}+\bar{S}_k \quad (2)$$

$$\frac{\partial(\rho h\tilde{\varepsilon})}{\partial t}+div(\rho h\tilde{\varepsilon}\vec{v})=div(h(\mu+\frac{\tilde{\mu}_t}{\sigma_\varepsilon})\mathbf{grad}\tilde{\varepsilon})+C_1hP_k\frac{\tilde{\varepsilon}}{\tilde{k}}-C_2\rho h\frac{\tilde{\varepsilon}^2}{\tilde{k}}+\rho hP_{\varepsilon v}+\bar{S}_\varepsilon \quad (3)$$

where $\bar{S}_k$ and $\bar{S}_\varepsilon$ are the source-sink terms, $P_k=\tilde{\mu}_t\left[2\left(\frac{\partial\bar{u}}{\partial x}\right)^2+2\left(\frac{\partial\bar{v}}{\partial y}\right)+\left(\frac{\partial\bar{u}}{\partial y}+\frac{\partial\bar{v}}{\partial x}\right)^2\right]$ is the production of turbulent kinetic energy due to interactions of turbulent stresses with horizontal mean velocity gradients, $\tilde{\mu}_t$ can be expressed as:

$$\tilde{\mu}_t=\rho C_\mu\tilde{k}^2/\tilde{\varepsilon} \quad (4)$$

where $\tilde{k}$ and $\tilde{\varepsilon}$ stand for depth-averaged turbulent kinetic energy parameter and dissipation rate parameter of $\tilde{k}$. The values of empirical constants C_μ, σ_k, σ_ε, C_1 and C_2 in Equations. (2 to 4) are the same as the 'standard' *k-ε* model, that is, equal to 0.09, 1.0, 1.3, 1.44 and 1.92, respectively. The additional source terms P_{kv} and $P_{\varepsilon v}$ in Equations (2) and (3) are mainly produced by the vertical velocity gradients near the bottom, and can be expressed as follows:

$$P_{kv}=C_ku_*^3/h,\quad P_{\varepsilon v}=C_\varepsilon u_*^4/h^2 \quad (5)$$

where the local friction velocity u_* is equal to $\sqrt{C_f\left(\bar{u}^2+\bar{v}^2\right)}$, the empirical constants C_k and C_ε for open channel flow and rivers are:

$$C_k=1/\sqrt{C_f},\quad C_\varepsilon=C_2C_\mu^{1/2}/(C_f^{3/4}\times e^{*1/2}) \quad (6)$$

where C_f represents an empirical friction factor and e^* is the dimensionless diffusivity of the empirical formula for undisturbed channel/river flows $\tilde{\mu}_t=e^*U_*h$ with U_* being the global friction velocity.

In 1989, the author of the present paper and his colleague developed a depth-averaged second-order closure model (Yu and Zhang 1989), $\tilde{k}$ - $\tilde{w}$, which originated from the revised k - w model developed by Ilegbusi and Spalding (1982) and has been adopted as the second turbulence closure model in the paper. The two extra transport equations (that is, the $\tilde{k}$ - equation and $\tilde{w}$ -equation) should be:

$$\frac{\partial(\rho h\tilde{k})}{\partial t}+div(\rho h\tilde{k}\vec{v})=div(h(\mu+\frac{\tilde{\mu}_t}{\sigma_k})\mathbf{grad}\tilde{k})+hP_k+\rho hP_{kv}-C_\mu\rho h\tilde{k}\tilde{w}^{1/2}+\bar{S}_k \quad (7)$$

$$\frac{\partial(\rho h\tilde{w})}{\partial t}+div(\rho h\tilde{w}\vec{v})=div(h(\mu+\frac{\tilde{\mu}_t}{\sigma_\varepsilon})\mathbf{grad}\tilde{w})+C_{1w}\tilde{\mu}_th(\mathbf{grad}\Omega)^2-C_{2w}\rho h\tilde{w}^{3/2}f+C_{3w}h\frac{\tilde{w}}{\tilde{k}}P_k+\rho hP_{wv}+\bar{S}_w \quad (8)$$

where $\bar{S}_k$ and $\bar{S}_w$ are the source-sink terms; function $f=1+C'_{2w}(\partial L/\partial x_i)$ and L is the characteristic distance of turbulence; Ω stands for mean movement vorticity. In $\tilde{k}$ - $\tilde{w}$ model, the turbulent viscosity is defined as:

$$\tilde{\mu}_t=\rho\tilde{k}^2/\tilde{w}^{1/2} \quad (9)$$

where $\tilde{w}$ is depth-averaged time-mean-square vorticity fluctuation parameter of turbulence. The transport equations (the $\tilde{k}$ -equation and $\tilde{w}$ -equation) should be solved in this model as well. The values of empirical constants C_μ, σ_k, σ_w, C_{1w}, C_{2w}, C'_{2w} and C_{3w} are the same as those of 'standard' *k-w* model, that is, equal 0.09, 1.0, 1.0, 3.5, 0.17, 17.47 and 1.12, respectively. The corresponding additional source terms P_{kv} and P_{wv}, also mainly due to the vertical velocity gradients near the bottom, and can be expressed as:

$$P_{kv}=C_ku_*^3/h,\quad P_{wv}=C_wu_*^3/h^3 \quad (10)$$

which were given by Yu and Zhang (1989). The empirical constants C_w for open channel flow and rivers can be written as:

$$C_w=C_{2w}/\left(C_\mu^{3/2}\times C_f^{3/4}\times e^{*3/2}\right) \quad (11)$$

Recently, the author has established a new depth-averaged model, $\tilde{k}$ - $\tilde{\omega}$, based on the most common standard k - ω model (in which ω is the special dissipation rate), originally introduced by Saffman (1970) but popularized by Wilcox (1998). The standard k - ω turbulence model has been used in engineering researches (Riasi et al., 2009; Kirkgoz et al., 2009). In the depth-averaged $\tilde{k}$ - $\tilde{\omega}$ turbulence model, the turbulent viscosity is expressed by:

$$\tilde{\mu}_t=\rho\tilde{k}/\tilde{\omega} \quad (12)$$

where $\tilde{\omega}$ is the special dissipation rate parameter of turbulence kinetic energy in the depth-averaged sense.

As the used third two-equation closure turbulence model, $\tilde{k}$ and $\tilde{\omega}$ are determined by also solving two extra transport equations, that is, the $\tilde{k}$ - equation and $\tilde{\omega}$ - equation (Yu and Yu, 2009):

$$\frac{\partial(\rho h\tilde{k})}{\partial t}+div(\rho h\tilde{k}\vec{v})=div(h(\mu+\frac{\tilde{\mu}_t}{\sigma_k^*})\mathbf{grad}\tilde{k})+hP_k-\rho\beta^* h\tilde{k}\tilde{\omega}+\rho hP_{kv}+\bar{S}_k \quad (13)$$

$$\frac{\partial(\rho h\tilde{\omega})}{\partial t}+div(\rho h\tilde{\omega}\vec{v})=div(h(\mu+\frac{\tilde{\mu}_t}{\sigma_\omega^*})\mathbf{grad}\tilde{\omega})+\alpha h\frac{\tilde{\omega}}{\tilde{k}}P_k-\rho h\beta\tilde{\omega}^2+\rho hP_{\omega v}+\bar{S}_\omega \quad (14)$$

where $\bar{S}_k$ and $\bar{S}_\omega$ are the source-sink terms. The values of empirical constants α, β, β^*, σ_k^*, and σ_ω^* in Equation (13) through Equation (14) are the same as in the 'standard' k - ω model: 5/9, 0.075, 0.9, 2, and 2, respectively. According to the dimensional analysis, the additional source terms P_{kv} in the *k*-equation (13) and $P_{\omega v}$ in the ω-equation (14) are:

$$P_{kv}=C_k u_*^3/h,\quad P_{\omega v}=C_\omega u_*^2/h^2 \quad (15)$$

while the empirical constant C_ω for open channel flow and rivers can be expressed as:

$$C_\omega=\beta/(C_\mu\times e^*\times C_f^{1/2}) \quad (16)$$

Except for the widely investigated and applied classical depth-averaged $\tilde{k}$ - $\tilde{\varepsilon}$ turbulence model, the author also adopts the $\tilde{k}$ - $\tilde{w}$ and $\tilde{k}$ - $\tilde{\omega}$ models, mentioned above, to close the fundamental governing equations in the current computations. The developed mathematical model and turbulence models by the author have been numerically investigated with laboratorial and site data for different flow situations (Yu and Zhang, 1989; Yu and Righetto, 1998; Yu and Yu, 2009). In the established mathematical model, the original empirical constants of three depth-averaged turbulence models, suggested by their authors, are employed and do not been changed never.

GRID GENERATION

One reach of The Solimões River (the section of the upper Amazon River), near The Lago Gabriel, northwestern Brazil, has been computed by using the developed *grid-generator* and *flow-solver*, written by FORTRAN Language. In this simulation, one tributary feeds into the river reach on the right side. The confluent tributary has a concentration difference in comparison with the mainstream, caused by the humus in tropical rain forest (produced by tropic rains). With the help of a developed *interface*, it is possible to determine the scale of digital map (the *Google* map), to collect conveniently geometrical data, including the positions of two curved riversides and two boundaries of one island as well as the location of the tributary in the computational domain, and finally to generate one text file. This file contains all of messages, which illustrate necessary control variables and characteristic parameters, including those on four exterior boundaries (west inlet section, east outlet section, south and north riversides) and two interior boundaries (south and north boundaries of the island), and can be read by the *grid-generator* for generating the expectant coarse and fine grids (two levels' grids).

Figure 1 demonstrates the digital map, on which the developed *interface* has divided the interested computational river reach into 43 sub-reaches with 44 short cross-river lines. It is noticed that the cross-river lines between the riverside and island boundary have been redrawn, in order to involve the island configuration. Figure 2 presents the generated non-orthogonal body-fitted coarse grid, with the resolution of 203 nodal points in *i*-direction and 18 nodal points in *j*-direction, respectively. In the generated mesh, the nodal points in transversal grid lines are uniform. The total length of the calculated river reach is 39.931 km. The flow direction is from the south and west to the north and east. The tributary feeds into the mainstream on the south riverside, with the numbers of nodal points from *i*=75 to *i*=80 on the coarse grid. The island starts at (*i*=35, *j*=5) and ends at (*i*=59, *j*=5) on the same mesh. The developed *grid-generator* generated two layers' grids, on which all of geometric data, necessary in the later calculation of flow and transport, must be stored and then can be read by the developed *flow-solver*. The resolution of the fine grid is 403 × 34, displayed on Figure 3. This means that one volume cell on the coarse grid was divided into four volume cells on the fine grid. Figure 4 represents the bottom topography on coarse grid. During the calculation, the variation of bottom topography was considered.

SOLUTIONS OF FLOW AND SIDE DISCHARGE

The behaviors of flows and contaminant transport were simulated by using the developed flow-solver, in which the SIMPLE (Semi-Implicit Method for Pressure-Linked Equation) algorithm for FVA (Finite Volume Approach), Guass' divergence theorem, ILU (Incomplete Lower-Upper) decomposition, PWIM (Pressure Weighting Interpolation Method), SIP (Strongly Implicit Procedure), under relaxation and multi-grid iterative method have been used. The fundamental governing equations were solved at each grid level in the following sequence: two

momentum equations ($\bar{u}$-equation and $\bar{v}$-equation), one pressure-correction equation (p'-equation), one concentration transport equation ($\bar{C}_i$-equation), and two turbulence transport equations ($\tilde{k}$-equation and $\tilde{\varepsilon}$-equation; or $\tilde{k}$

Figure 1. *Google* map, plotted by *interface*.

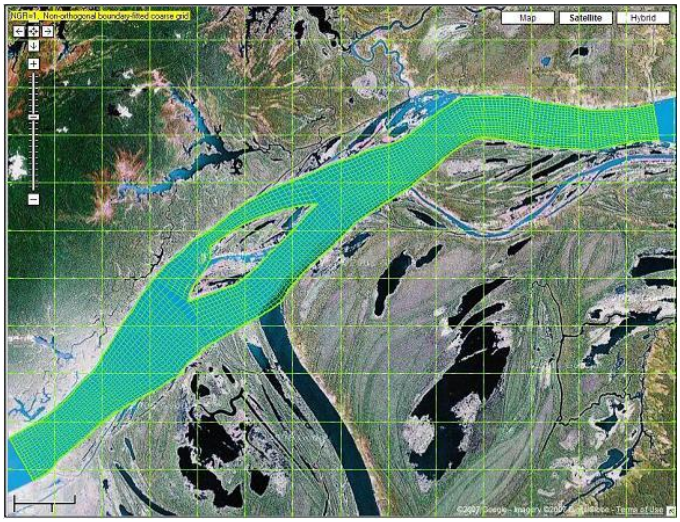

Figure 2. Coarse grid.

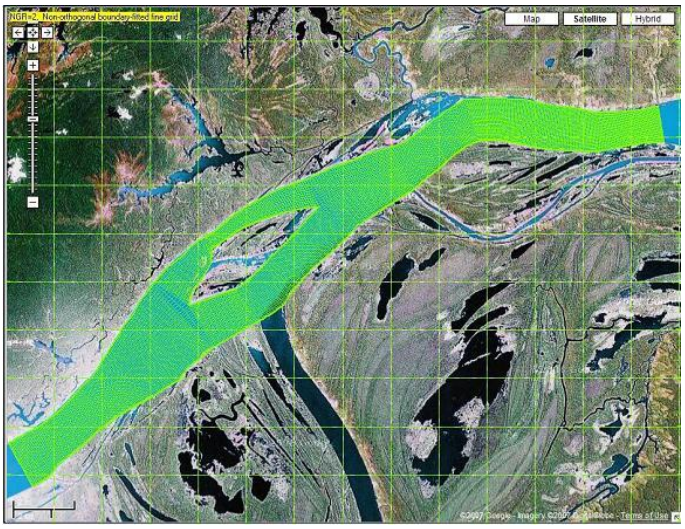

Figure 3. Fine grid.

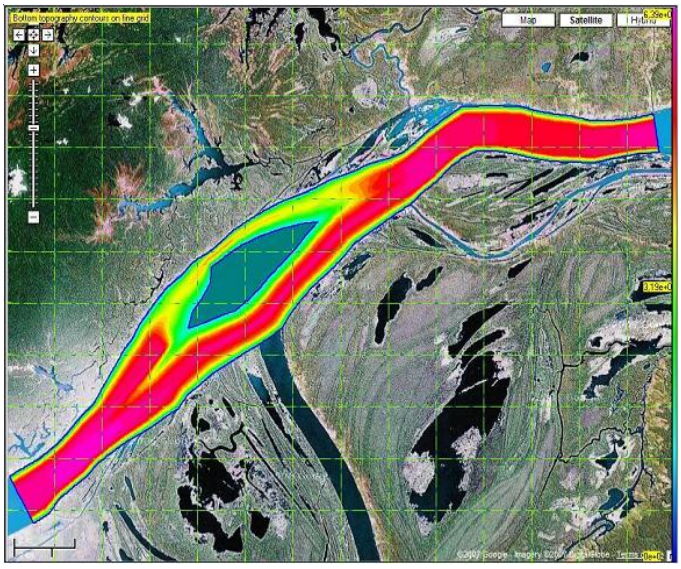

Figure 4. Bottom topography.

- equation and $\tilde{w}$-equation; or $\tilde{k}$-equation and $\tilde{\omega}$-equation), respectively.

The calculated main stream flow-rate is 20,000 m^3/s, while the width, area and mean water-depth of the inlet section are 2,584 m, 13,501.5 m^2 and 5.23 m. The empirical friction factor (C_f) equals 0.00313. The tributary flow-rate and concentration difference are 800 m^3/s and 100 mg/L, respectively. Three depth-averaged two-equation closure turbulence models, that is, $\tilde{k}$ - $\tilde{\varepsilon}$, $\tilde{k}$ - $\tilde{w}$ and $\tilde{k}$ - $\tilde{\omega}$ models, are adopted to close the quasi-3D hydrodynamic model. The turbulence parameters at the inlet sections can be calculated by empirical formulae, that is, $\tilde{k}_0$, $\tilde{\varepsilon}_0$, $\tilde{w}_0$, $\tilde{\omega}_0$ are 0.0617 m^2/s^2, 0.00145 m^2/s^3,

0.358/s^2, 0.262/s, and $\tilde{k}_{tri}$, $\tilde{\varepsilon}_{tri}$, $\tilde{w}_{tri}$, $\tilde{\omega}_{tri}$ equal 0.0692 m^2/s^2, 0.00257 m^2/s^3, 0.3394/s^2, 0.412/s, respectively. On the outlet section, the variables satisfy constant gradient condition. The wall function approximation has been used for determining the values of velocity components and turbulence parameters at the nodal points in the vicinity of riversides and the boundaries of island.

Due to the existence of the island in mesh, the values of the under-relaxation factors for velocity components, pressure, concentration and two turbulence parameters in the multi-grid iterative method may be lower than those while no exists any island in the domain. However, in this example, these factors are still 0.6, 0.6, 0.1, 0.7, 0.7 and 0.7, respectively. The maximum allowed numbers of inner iteration for solving velocity components, pressure, concentration and two turbulence parameters are 1, 1, 20, 1, 1 and 1. The convergence criterions for inner iteration are 0.1, 0.1, 0.01, 0.1, 0.01 and 0.01, respectively. The α parameter of the Stone's solver is

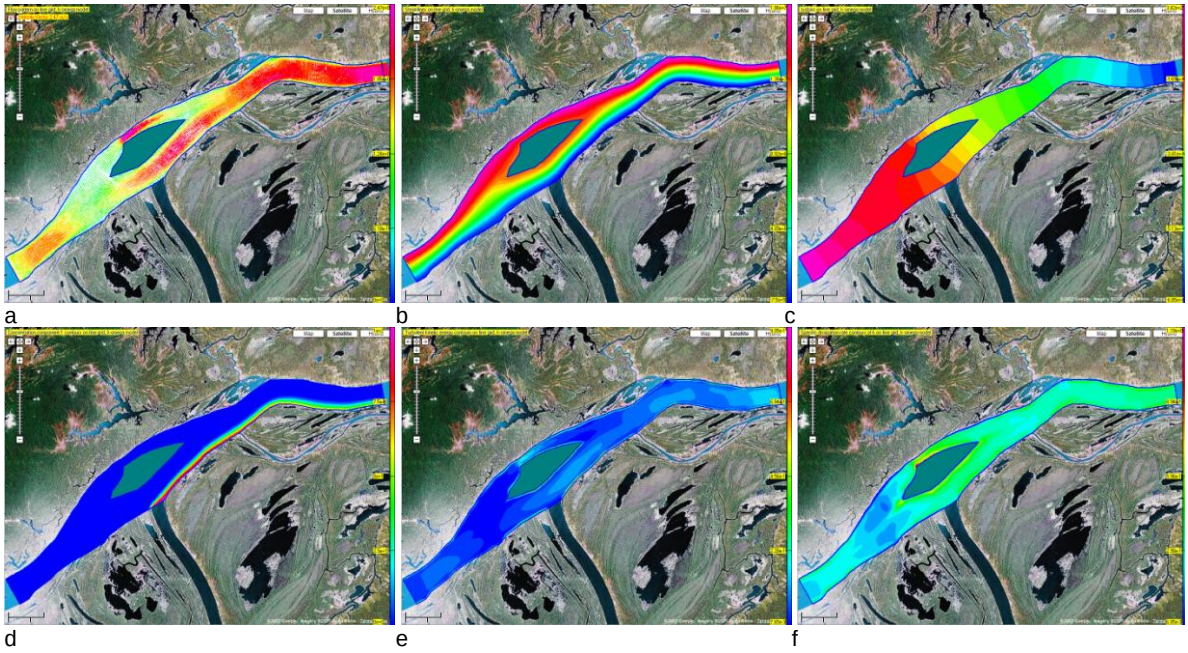

Figure 5. A part of results, calculated by $\tilde{k}$ - $\tilde{\omega}$ model.

equal to 0.92. The normalize residuals for solving velocity, pressure, concentration and turbulence parameter fields are all less than pre-determined convergence criterion (1.e-4).

The simulation obtained various distributions of flow, pressure, concentration and turbulence parameter, which are useful to analyze interested problems in engineering. A part of results, simulated by using $\tilde{k}$ - $\tilde{\varepsilon}$, $\tilde{k}$ - $\tilde{w}$ and $\tilde{k}$ - $\tilde{\omega}$ models on the fine grid, are presented from Figures 5 to 9. Figure 5 display the results, calculated by using $\tilde{k}$ - $\tilde{\omega}$ model closure, with a: flow pattern, b: flow field, c: pressure field, d: concentration field, e: $\tilde{k}$ distribution and f: $\tilde{\omega}$ distribution, respectively. Figure 5d illustrates that the pollutant plume well develops along the right riverside at the lower reach of inpouring section. The distributions of the same depth-averaged physical variable and turbulence parameter $\tilde{k}$, calculated by $\tilde{k}$ - $\tilde{\varepsilon}$ and $\tilde{k}$ - $\tilde{w}$ turbulence models, are similar to Figures 5a-5e. Figures 6a, 6b and 6c demonstrate the three-dimensional distributions of turbulence parameter $\tilde{k}$, calculated by using these three depth-averaged turbulence models. They are quite similar each other, with the maximum values: 0.8903 m^2/s^2 for $\tilde{k}$ - $\tilde{\varepsilon}$ modeling (6a), 0.8894 m^2/s^2 for $\tilde{k}$ - $\tilde{w}$ modeling (6b) and 0.9048 m^2/s^2 for $\tilde{k}$ - $\tilde{\omega}$ modeling (6c), respectively. Figures 7a, 7b and 7c present the three-dimensional distributions of turbulence parameters $\tilde{\varepsilon}$, $\tilde{w}$ and $\tilde{\omega}$, which are different each other, because of the different definitions of the used second turbulence parameter in current computations. Actually, the $\tilde{\varepsilon}$ value, shown in Figure 7a, ranges only from 9.5e-6 to 0.0223 m^2/s^3; however, the $\tilde{w}$ parameter and $\tilde{\omega}$ parameter range from 4.76e-5 to 1.5038/s^2 and from 0.685e-2 to 1.1857/s, shown in Figure 7b and Figure 7c respectively. Figures

8a, 8b and 8c illustrate the three-dimensional distributions of effective viscosity $\tilde{\mu}_{\text{eff}}$, while the depth-averaged turbulent eddy viscosity $\tilde{\mu}_{\text{t}}$ was calculated by using Equation (4) for $\tilde{k}$ - $\tilde{\varepsilon}$ modeling (8a), Equation (9) for $\tilde{k}$ - $\tilde{w}$ modeling (8b) and Equation (12) for $\tilde{k}$ - $\tilde{\omega}$ modeling (8c), respectively. Basically, they are similar each other, specially for $\tilde{k}$ - $\tilde{\varepsilon}$ and $\tilde{k}$ - $\tilde{w}$ modeling, while the maximum values of $\tilde{\mu}_{\text{eff}}$ are 8910.3 Pa.s (8a) and 8907.5 Pa.s (8b); but the same value for $\tilde{k}$ - $\tilde{\omega}$ moding is 9000.9 Pa.s (8c). Figure 9 shows the distributions of the production term of turbulent kinetic energy, with the maximum values of P_k 2.4979 Pa.m/s for $\tilde{k}$ - $\tilde{\varepsilon}$ modeling (9a), 2.4976 Pa.m/s for $\tilde{k}$ - $\tilde{w}$ modeling (9b) and 2.522 Pa.m/s for $\tilde{k}$ - $\tilde{\omega}$ modeling (9c). They are also similar each other. Figure 10 displays the concentration configuration near the tributary outlet, on which a concentration contour (fine blue line) with 20 mg/L

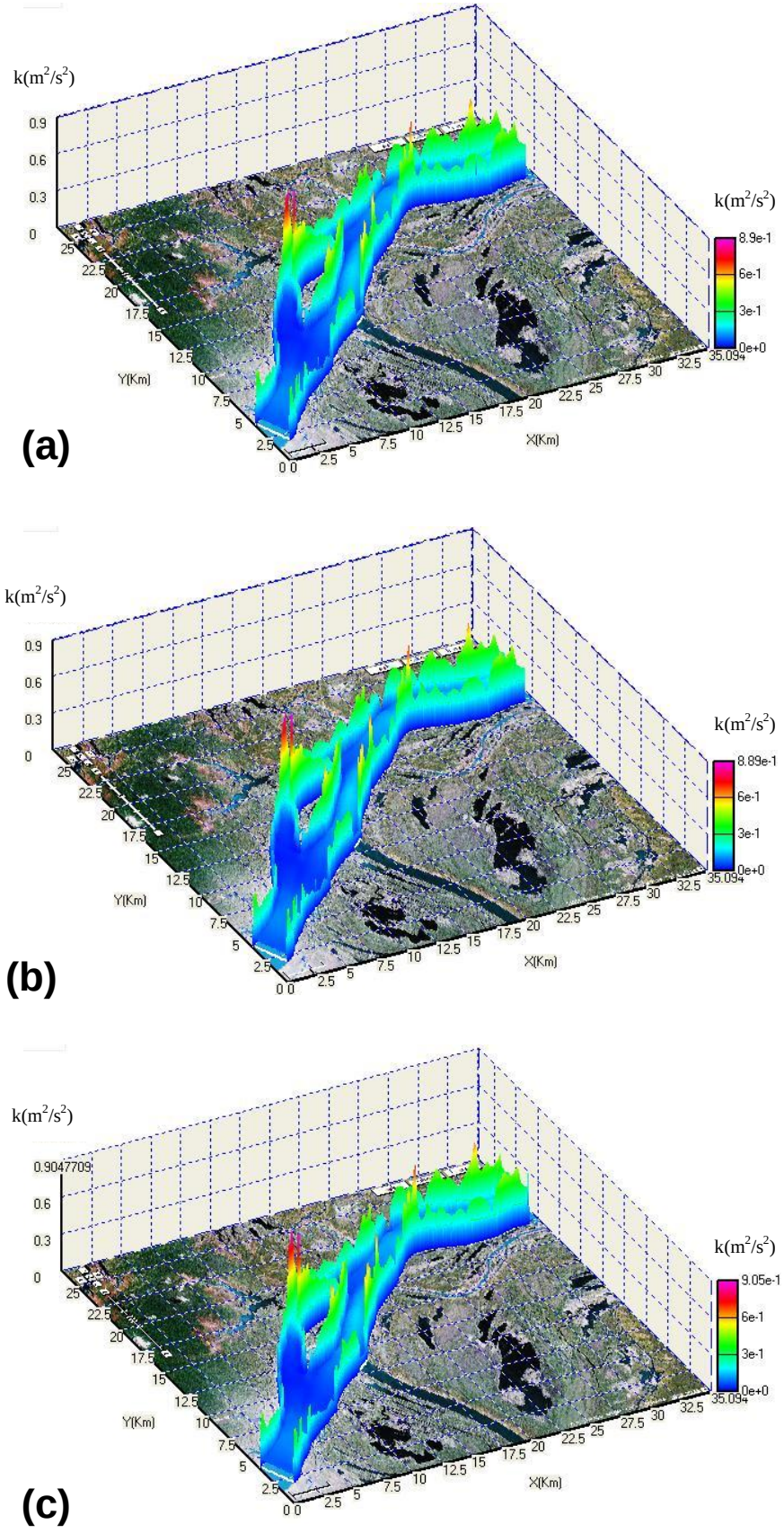

Figure 6. 3D $\tilde{k}$ distributions, calculated by $\tilde{k}$ - $\tilde{\varepsilon}$, $\tilde{k}$ - $\tilde{w}$ and $\tilde{k}$ - $\tilde{\omega}$ models.

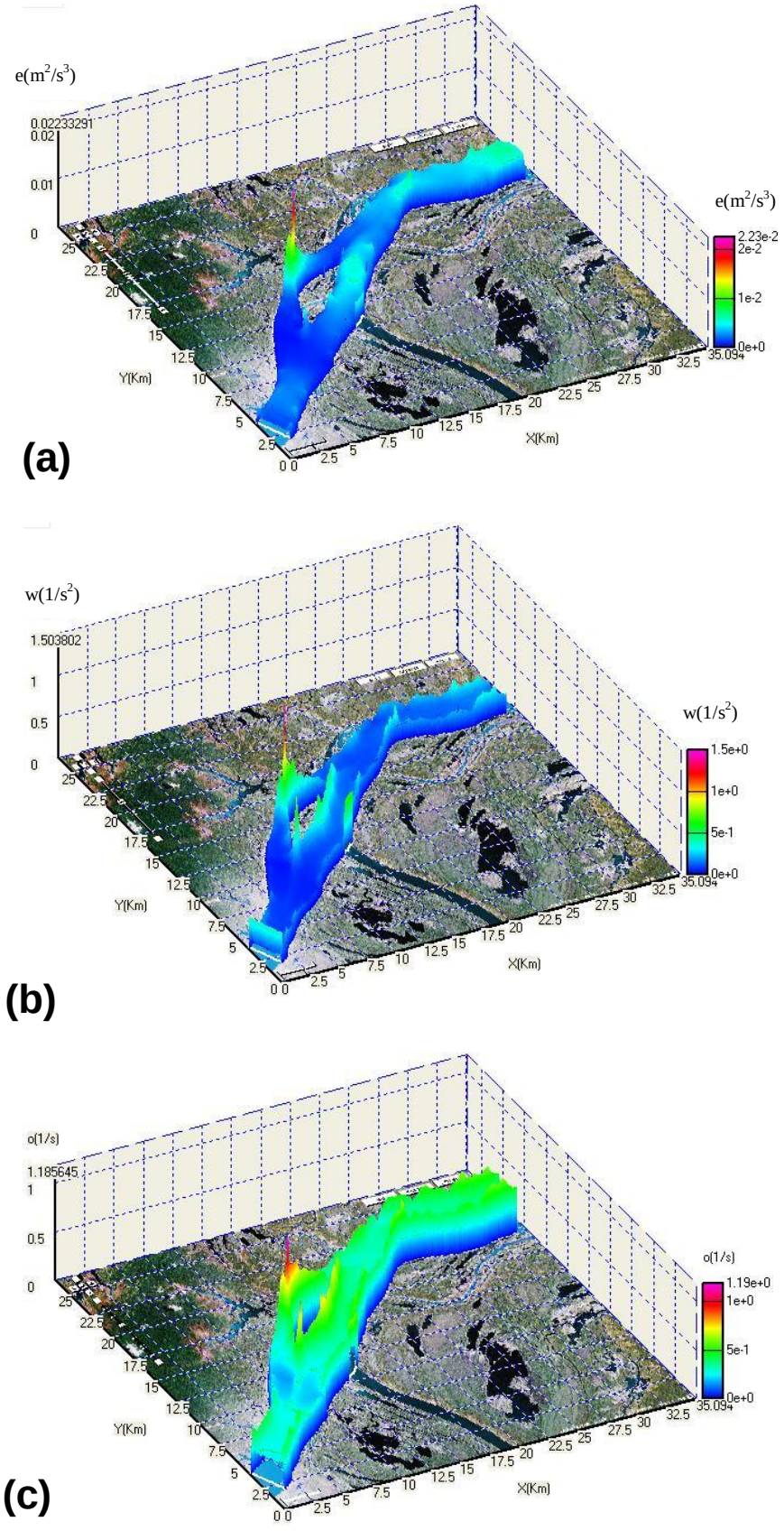

Figure 7. 3D $\tilde{\varepsilon}$, $\tilde{w}$ and $\tilde{\omega}$ distributions.

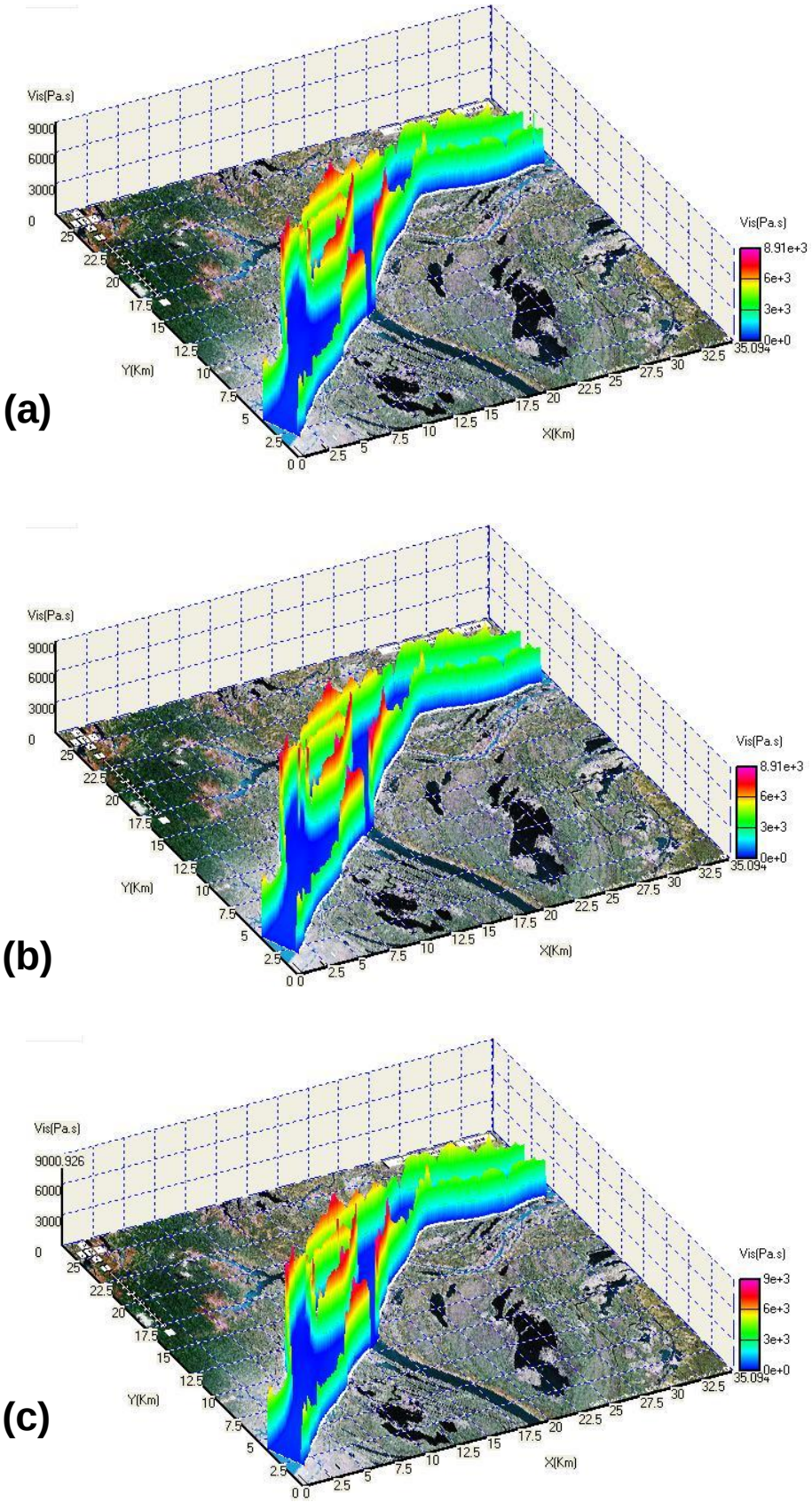

Figure 8. 3D $\tilde{\mu}_{\text{eff}}$ distributions, calculated by $\tilde{k}$ - $\tilde{\varepsilon}$, $\tilde{k}$ - $\tilde{w}$ and $\tilde{k}$ - $\tilde{\omega}$ models.

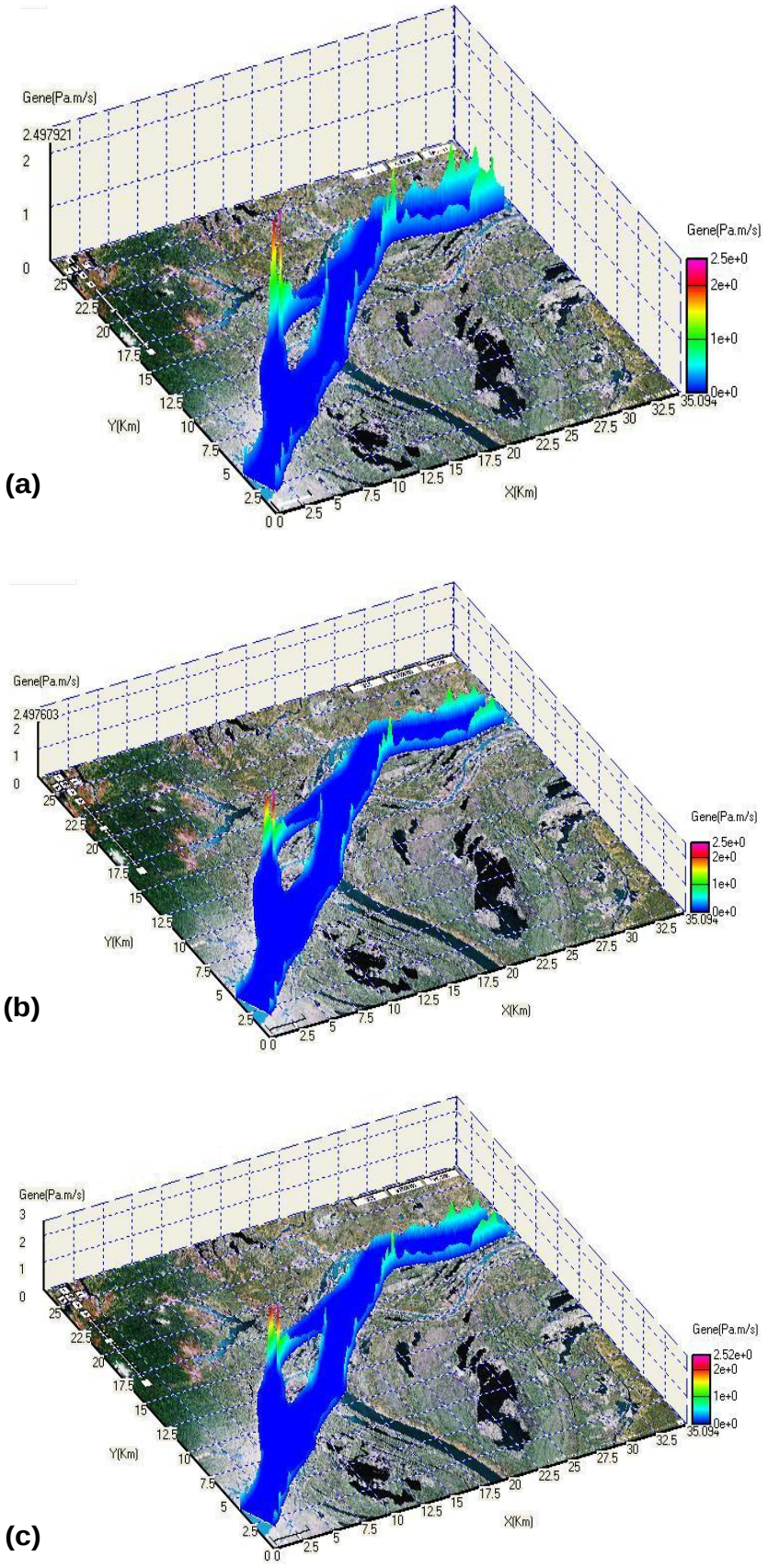

Figure 9. P_k distributions, calculated by $\tilde{k}$ - $\tilde{\varepsilon}$, $\tilde{k}$ - $\tilde{w}$ and $\tilde{k}$ - $\tilde{\omega}$ models.

Figure 10. Concentration near tributary outlet.

calculated by the depth-averaged $\tilde{k}$ - $\tilde{\omega}$ turbulence models, was plotted. It is clear that the simulated depth-averaged isoline, however, is quite coincident with the configuration of pollution plume, shown on the satellite map. Figure 11 displays the comparison of concentration profiles along the centers of the volume cells at *j*=2 on the fine grid (that is, along a curved line from the inlet to the outlet near the south riverside), calculated by the depth-averaged $\tilde{k}$ - $\tilde{\varepsilon}$, $\tilde{k}$ - $\tilde{w}$, and $\tilde{k}$ - $\tilde{\omega}$ turbulence models, respectively. Figure 12 shows the comparison between turbulence parameters $\tilde{\varepsilon}$, $\tilde{w}$ and $\tilde{\omega}$ on the transversal section at *i*=350 of the fine grid, calculated by the three depth-averaged turbulence models: $\tilde{k}$ - $\tilde{\varepsilon}$, $\tilde{k}$ - $\tilde{w}$, and $\tilde{k}$ - $\tilde{\omega}$, respectively. The orders of magnitudes of $\tilde{\varepsilon}$, $\tilde{w}$ and $\tilde{\omega}$, used in three turbulence models, have significant differences in deed.

PLUME DEVELOPMENT AT THE BEGINNING OF DISCHARGE

In order to well understand the development process of contaminant plume, a special simulation was performed by using $\tilde{k}$ - $\tilde{\omega}$ model closure for the case described as follows. Supposing the concentration of tributary firstly to equal zero, and then, the value of concentration instantaneously reaches 100 mg/L at Time=0, while the flow-rates, either of main stream or of tributary, keep constant. Figures 13a-h illustrate the plume development and variation in the lower reach of tributary outlet section, where Figure 13a presents the situation of clean water confluence; Figures 13b-h display the process of contaminant in pouring and plume development, with an equal time difference Δt each other.

DISCUSSION

Two-equation turbulence models are one of the most common type of turbulence models. The so-called 'standard' two-equation closure turbulence models cannot be directly adopted in depth-averaged modeling. Till now, the vast majority of quasi 3-dimensional numerical tools in the world merely can provide depth-averaged $\tilde{k}$ - $\tilde{\varepsilon}$ turbulence model for users, which appears already beyond 30 years. However, current advanced Computational Fluid Dynamics (CFD) software for standard 2D and 3D modeling can provide several, even up to dozens of two-equation closure turbulence models, because there is non-existent a 'universal' turbulence closure model in the theory of turbulence modeling. Moreover, two-equation turbulence models are also very much still an active area of research and new refined two-equation models are still being developed. This situation in the area of quasi-3D modeling should be changed as soon as possible.

At present, the *k-ω* model, just like the *k-ε* model, has become industry standard model and is commonly used for most types of engineering problems. Therefore, the establishment of depth-averaged $\tilde{k}$ - $\tilde{\omega}$ turbulence model and the numerical investigation and comparison with existing depth-averaged turbulence models, presented in this paper, are quite significant.

Two levels of grids were used in this simulation: a coarse grid and a fine grid. The simulation on these two grids can satisfy the simulation demand. For example, by setting the number of grid levels at three, computations not only on coarse and fine grids but also on finest grid can be realized. The selection of the number of grid levels depends on the solved problems and computational requirements.

The solved depth-averaged concentration variable in the current computation is the concentration difference of humus between the confluent tributary black water and the main stream clean water (100 mg/L). However, other contaminant indexes of discharged black water, such as COD and BOD, can also be considered the solved variable. The developed numerical tool of this study possesses the ability to simultaneously solve two concentration components in one calculation, which are caused by industrial, domestic, and natural discharges.

Figure 6 demonstrates that the distributions of turbulence parameter $\tilde{k}$, calculated by three turbulence models, vary strongly in the computational domain, but quite similar to one another. However, the characteristics of the distributions of turbulence parameters $\tilde{\varepsilon}$, $\tilde{w}$ and

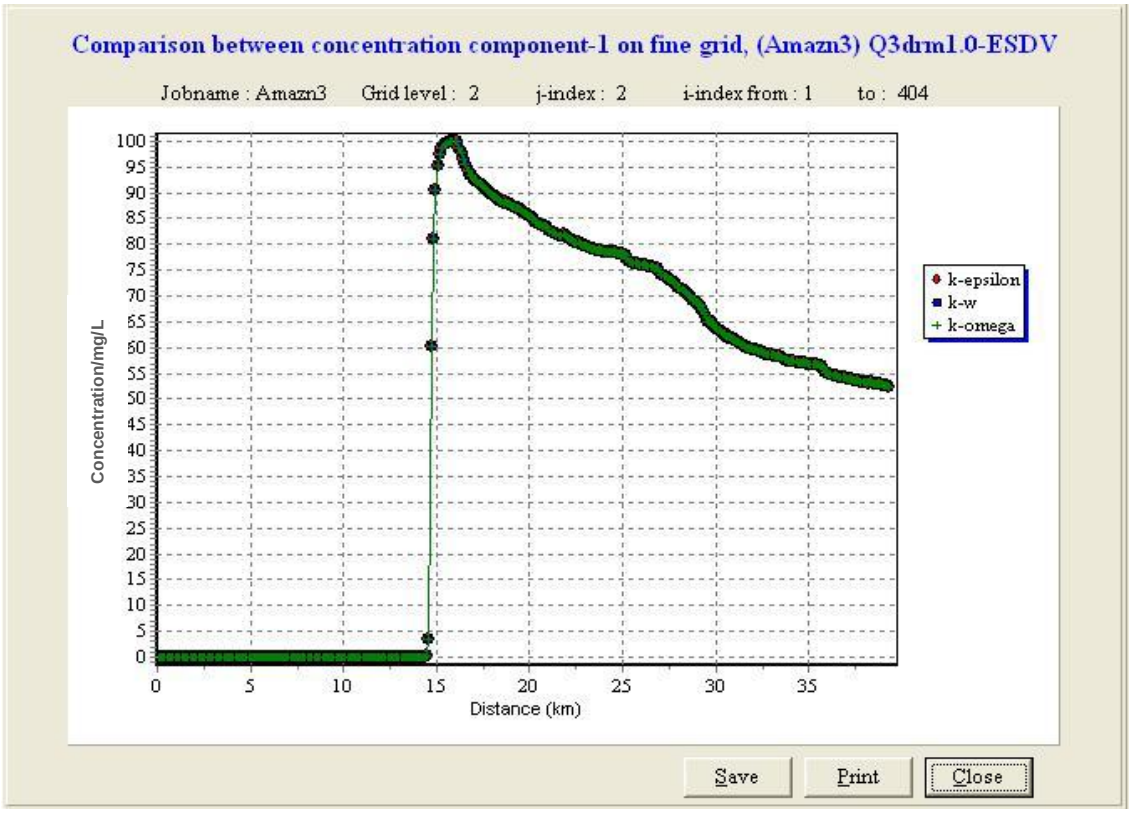

Figure 11. Concentrations at *j*=2.

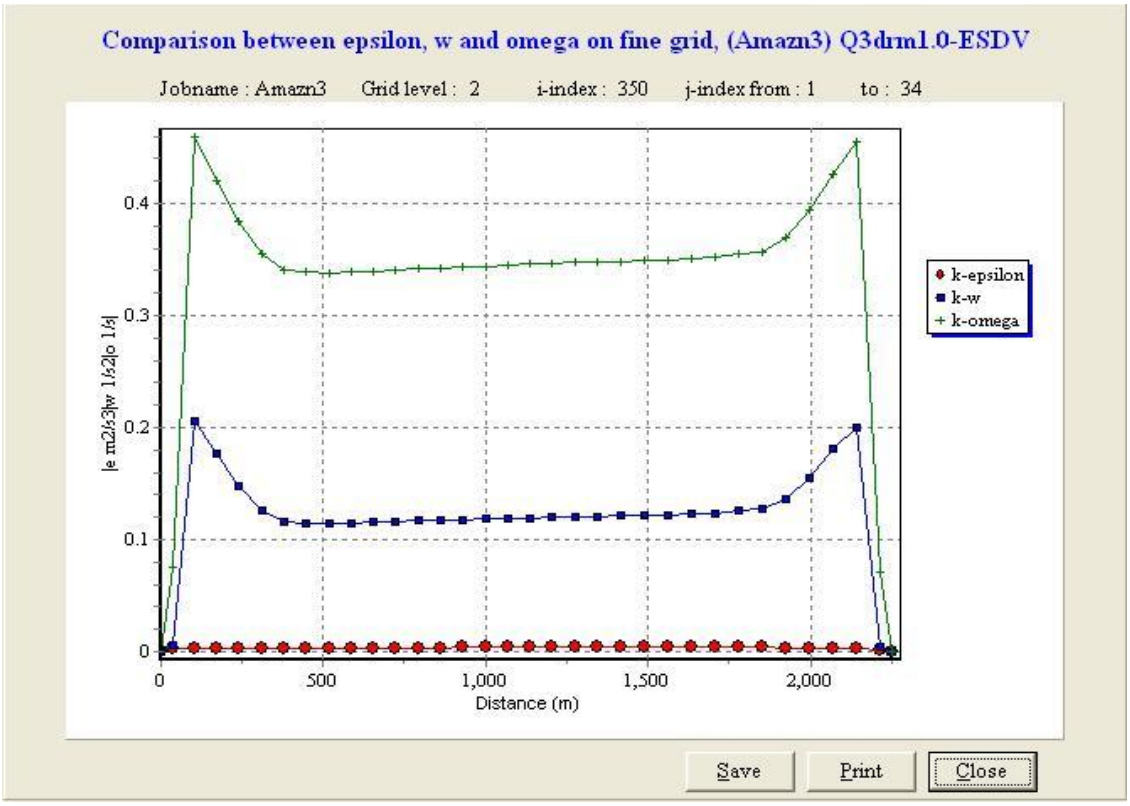

Figure 12. Parameters $\tilde{\varepsilon}$, $\tilde{w}$, $\tilde{\omega}$ at *i*=350.

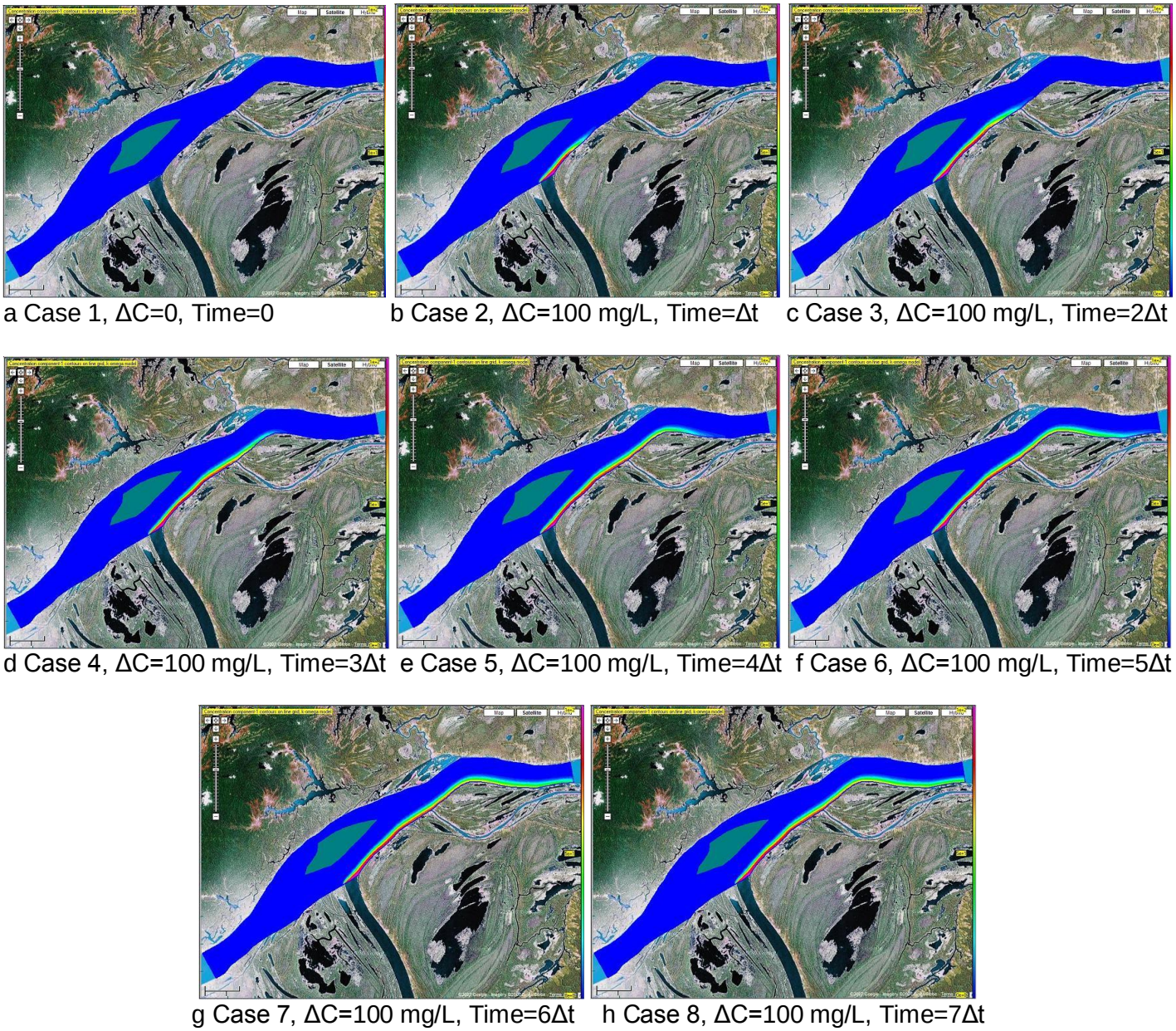

Figure 13. Plume development.

$\tilde{\omega}$, shown in Figures 7a, 7b and 7c, respectively, are different from one another, though they also vary sharply.

The calculated effective viscosity $\tilde{\mu}_{\text{eff}}$, presented in Figures 8a, 8b and 8c, also varies strongly. In fact, the eddy viscosity changes from point to point in the computational domain, especially in the areas near two riversides and two island boundaries. To solve the problems of contaminant transport caused by side discharge, for example, the pollutant plume usually develops along a region near riverside (see Figure 5d), where $\tilde{\mu}_{\text{t}}$ (or $\tilde{\mu}_{\text{eff}}$) actually varies much strongly (Figure 8). This means that $\tilde{\mu}_{\text{t}}$ should be precisely calculated using suitable higher-order turbulence closure models with higher precision, and cannot be considered as an adjustable constant.

Figure 11 shows that the computational concentration profiles along the south riverbank, either from the $\tilde{k}$ - $\tilde{\varepsilon}$ model, from the $\tilde{k}$ - $\tilde{w}$ model, or from the $\tilde{k}$ - $\tilde{\omega}$ model, only have a quite small difference from one another, in the range of no more than 0.5 mg/L. This means that the three utilized depth-averaged two-equation closure turbulence models almost have the same ability to

simulate contaminant plume distributions along riverbank (Figure 10). The results of this study also coincide with the result of previous research that the depth-averaged two-equation closure turbulence closure models are all suitable for modeling strong mixing turbulence. However, the abilities and behaviors of different depth-averaged two-equation closure turbulence models for rather weak mixing, also often encountered in engineering, should be further investigated.

Except for the different definitions of transported variables $\tilde{\varepsilon}$, $\tilde{w}$ and $\tilde{\omega}$, the order of magnitude of turbulence parameter $\tilde{\varepsilon}$ is smaller than the order of magnitude of $\tilde{w}$, and much smaller than the order of magnitude of $\tilde{\omega}$. It should be noticed that three transported variables $\tilde{\varepsilon}$, $\tilde{w}$ and $\tilde{\omega}$ all appear in the denominators of Equations (4), (9) and (12), which were used to calculate turbulent eddy viscosity $\tilde{\mu}_t$. For numerical simulation, the occurrence of numerical error is unavoidable, especially in the region near irregular boundary. It is clear that a small numerical error, caused by solving $\tilde{\varepsilon}$-equation, for example, will bring on larger error for calculating eddy viscosity than the same error caused by solving the other two equations ($\tilde{w}$-equation and $\tilde{\omega}$-equation). Without doubt, the elevation of the order of magnitude of the used second turbulence parameter, reflecting the advance of two-equation closure models, provides a possibility for users to improve their computational precision. The insufficiency of classical depth-averaged $\tilde{k}$ - $\tilde{\varepsilon}$ turbulence model may be avoided by adopting other turbulence models that have appeared recently, such as the $\tilde{k}$ - $\tilde{\omega}$ model.

The developed *Graphical User Interface* of Q3drm1.0 software can be used in various Windows-based microcomputers. The pre- and post-processors of this numerical tool, supported by a powerful self-contained map support tool together with a detailed help system, can help the user to easily compute the flows and contaminant transport behaviors in natural waters, closed by using three different depth-averaged two-equation turbulence models, and to draw and analyze two- and three-dimensional graphics of computed results.

REFERENCES

Cea L, Pena L, Puertas J, Vázquez-Cendón ME, Peña E (2007). Application of several depth-averaged turbulence models to simulate flow in vertical slot fishways. J. Hydraul. Eng. 2:160-172.

Chapman RS, Kuo CY (1982). A Numerical Simulation of Two-Dimensional Separated Flow in a Symmetric Open-Channel Expansion Using the Depth-Integrated Two Equation (k-ε) Turbulence Closure Model. Department of Civil Engineering, Virginia Polytechnic Institute and State University, Blacksburg, VA, Rep. 8202.

Choi M, Takashi H (2000). A numerical simulation of lake currents and characteristics of salinity changes in the freshening process. J. Japan Soc. Hydrol. Water Resourc. 6:439-452 (In Japanese).

Ferziger JH, Peric M (2002). Computational Methods for Fluid Dynamics, 3rd Edition. Berlin: Springer.

Hua ZL, Xing LH, Gu L (2008). Application of a modified quick scheme to depth-averaged κ–ε turbulence model based on unstructured grids. J. Hydrodyn. Ser. B4:514-523.

Ilegbusi JO, Spalding DB (1982). Application of a New Version of the k-w Model of Turbulence to a Boundary Layer with Mass Transfer. CFD/82/15. London: Imperial College.

Johnson HK, Karambas TV, Avgeris I, Zanuttigh B, Gonzalez-Marco D, Caceres I (2005). Modelling of waves and currents around submerged breakwaters. Coast. Eng. 10:949-969.

Kimura I, Uijttewaal WSJ, Hosoda T, Ali MS (2009). URANS computations of shallow grid turbulence. J. Hydraul. Eng. 135:118-131.

Kirkgoz MS, Akoz MS, Oner AA (2009). Numerical modeling of flow over a chute spillway. J. Hydraul. Res. 47:790-797.

Kwan S (2009). A Two-Dimensional Hydrodynamic River Morphology and Gravel Transport Model. Master (MASc) Degree Thesis. University of British Columbia.

Lee JT, Chan HC, Huang CK, Wang YM, Huang WC (2011). A depth-averaged two-dimensional model for flow around permeable pile groins. Int. J. Phys. Sci. 6:1379-1387.

Lunis M, Mamchuk VI, Movchan VT, Romanyuk LA, Shkvar EA (2004). Algebraic models of turbulent viscosity and heat transfer in analysis of near-wall turbulent flows. Int. J. Fluid Mech. Res. 31:60-74.

McGuirk JJ, Rodi W (1977). A Depth-Averaged Mathematical Model for Side Discharges into Open Channel Flow. SFB 80/T/88. Universität Karlsruhe.

Mei Z, Roberts AJ, Li ZQ (2002). Modelling the Dynamics of Turbulent Floods. SIAM J. Appl. Math. 63:423-458.

Riasi A, Nourbakhsh A, Raisee M (2009). Unsteady turbulent pipe flow due to water hammer using *k*–ω turbulence model. J. Hydraul. Res. 47:429-437.

Rodi W, Pavlovic RN, Srivatsa SK (1980). Prediction of flow pollutant spreading in rivers. Transport Models for Inland and Coastal Waters: Proceedings of Symposium on Predictive Ability, Berkeley: University of California Academic Press pp. 63-111.

Saffman PG (1970). A model for inhomogeneous turbulent flow. Proc. Roy. Soc. London. A317:417-433.

Vasquez JA (2005). Two Dimensional Finite Element River Morphology Model. Ph. D. Dissertation. University of British Columbia.

Wilcox DC (1998). Turbulence Modeling for CFD. La Canada: DCW Industries, Inc.

Yu LR, Righetto AM (1998). Tidal and transport modeling by using turbulence $\tilde{k}$ - $\tilde{w}$ model. J. Environ. Eng. 124:212-221.

Yu LR, Yu J (2009). Numerical research on flow and thermal transport in cooling pool of electrical power station using three depth-averaged turbulence models. Water Sci. Eng. 3:1-12.

Yu LR, Zhang SN (1989). A new depth-averaged two-equation ($\tilde{k}$ - $\tilde{w}$) turbulent closure model. J. Hydrodyn. Ser. B 1:47-54.